

APPLICATION OF GEOMETRIC MORPHOMETRICS TO THE STUDY OF POSTNATAL SIZE AND SHAPE CHANGES IN THE SKULL OF *Calomys expulsus*.

E. HINGST-ZAHER(*), L.F. MARCUS(**) AND R. CERQUEIRA(***)

* *Programa de pós graduação em Genética, Universidade Federal do Rio de Janeiro, RJ, Brasil*

** *Department of Biology, Queens College of the City University of New York and American Museum of Natural History.*

*** *Laboratório de Vertebrados, Departamento de Ecologia, Universidade Federal do Rio de Janeiro RJ, Brasil*

ABSTRACT - We analyzed ontogenetic patterns of landmarks for 169 laboratory-raised specimens of *Calomys expulsus*, at 0, 5, 10, 20, 30, 50, 100, 200, and 300 days of age, using two-dimensional geometric morphometrics. There is sexual dimorphism in size, with males smaller than females at earlier ages, but larger after 50 days. Differences in shape between sexes are strong only until 10 days of age, suggesting that shape is more constrained than size. Combining sexes, there is strong variation in size with age, reduced after 200 days, while most of the variation in shape occurs before 20 days. This dissociation is common for sigmodontine rodents, and might be the basis of heterochronic processes responsible for the morphological variation of this South American group. Centroid size does not show any reduction in the coefficient of variation over ages, while Procrustes distances within successive ages are reduced after 20 days. Uniform component and the more global partial warps explain most of the shape changes with age. Cranial and facial parts of the skull increase in size at different rates with a relative lengthening of the snout and decrease in height of the braincase. We were unable to detect a clear pattern of integration for the rostrum and braincase, besides that shown by landmark displacements.

Keywords: Rodentia, Sigmodontinae, ontogeny, growth.

INTRODUCTION

The mammalian skull has been an object of intense investigation, as it is a complex structure housing the brain and most of sensory organs. The developmental process of this structure is a source of information on the origin of morphological variation and its constraints, as well as phylogenetic history. Some general growth patterns can be inferred from studies on development of the mammalian **skull**: differences in timing and rates of growth between sexes and age classes, dissociation between size and shape, changes in direction of ontogenetic pathways, change of patterns of integration in

different parts of the skull, and reduction of phenotypic variance throughout ontogeny. The dissociation between size and shape allows for differences in timing of growth between sexes and age classes. If examined in a comparative (phylogenetic or ontogenetic) context one can detect heterochronic processes resulting in differences in the adult forms. This pattern is prevalent among mammals, as shown by many studies describing sexual dimorphism based on size rather than shape differences, either using traditional (Hingst, 1995; Voss et al., 1990) or geometric morphometrics (Fadda and Corti, this volume, Marcus et al., 1999).

Reduction of phenotypic variance during development is usually related to patterns of variance during growth, and commonly attributed to developmental regulation and canalization. Up to now, analysis of variance patterns in ontogenetic series has been performed mainly using traditional morphometrics (e.g. Tanner, 1963; Riska et al., 1984; Nonaka and Nakata, 1984; Hingst, 1995). Zelditch et al. (1993) in an ontogenetic study of *Sigmodon*, compare directions of variance reduction within each age to the direction of ontogenetic change in the mean form, using geometric morphometrics.

Developmental integration between different body parts is regulated by gene expression, mechanical interactions or by physiological requirements, and results in covariance of growth patterns between structures (Olson and Miller, 1958). Covariance of growth patterns is known to be constrained and to change during ontogeny for rodents (Zelditch and Carmichael, 1989; Atchley et al., 1985a, 1985b; Leamy et al., 1999) and primates (Cheverud, 1995). Studies on developmental integration have used factor analysis (Zelditch, 1988; Zelditch and Carmichael, 1989), finite element scaling with Mantel tests (Cheverud and Richtsmeier, 1986; Cheverud et al., 1989); distances using Mantel tests (Leamy et al., 1999); and more recently partial warps and thin plate splines in the spirit of geometric morphometrics (Zelditch et al., 1993; O'Higgins and Jones, 1998; Monteiro et al., 1999). Using traditional morphometrics (Marcus, 1990) one can not describe or represent the location of morphometric variability. Distance measurements made on the skull can only be analyzed by means of covariances and principal components, or by examining the total variability for a group of measurements describing a morphological complex. However, different parts of the skull vary with age, and also among individuals at the same age. Traditional morphometrics does not provide a comprehensive and graphic way of locating and comparing this vari-

ability. Size and shape, as defined from equivalent landmarks (placed at topologically equivalent structures) are the basis of a rich tool box provided by the "morphometric synthesis" (see Klingenberg and Bookstein, 1998; Bookstein, 1998; Marcus et al., 1993; Marcus et al., 1996; Corti, 1993; Rohlf and Bookstein, 1990). This synthesis is a comprehensive approach to describing and analyzing biological form (size+shape) in 3D organism space. It emphasizes geometric shape of the organism as summarized by landmarks. The advantage of geometric morphometrics over traditional morphometrics relies on the non-interconnectedness of landmarks, and the possibility of determining and representing the regions, from more localized to global, where there are differences in shape.

We explore the patterns of shape and size changes during ontogeny in 169 laboratory raised specimens of the sigmodontine rodent *Calomys expulsus*. This species is part of the South American radiation of murid rodents, and has a developmental pattern with no remarkable differences from other sigmodontines of similar size: young are born naked after 21 days of gestation with their eyes closed. They can be weaned around 21 days old, and start reproducing soon after, at about 25 days of age.

Our objective is to apply landmark morphometrics to describe ontogenetic growth patterns observed in *Calomys expulsus*

METHODS

We collected 37 specimens of *Calomys expulsus* at Fazenda Canoas, Minas Gerais, Brazil (16°50' S, 43°35' W, 800m). Sixteen nuliparous females and 21 sexually immature males were brought to the laboratory, kept under controlled conditions, and fed on mouse pellets and seeds. Couples were randomly paired and placed together in the same cage, so as to obtain offspring of known age. First generation males and females born in captivity were sacrificed at

Table 1 – Number of specimens of *C. expulsus* at each age for each sex.

Age (days)	0	5	10	20	30	50	100	200	300	400	Total
Males	1	3	5	11	12	13	12	12	12	0	81
Females	4	1	8	12	12	12	12	12	12	3	88
Total	5	4	13	23	24	25	24	24	24	3	169

the ages shown in Tab. 1. A preliminary analysis of variance of aligned coordinates and centroid sizes with age showed no differences between 300 (n=3) and 400 (n=24) days specimens, so we combined these two age classes. Within each age class, there is no more than one male and one female belonging to the same litter. This prevented having closely related individuals of the same sex in an age class, thus avoiding bias that could be introduced by genetic background and parity sequence. Skulls of 0 and 5 days old specimens were cleared and stained, while all older individuals were skeletonized.

We took black and white images of 169 skulls using an NTSC video camera and a Snappy capture hardware compatible with the parallel port of a PC. Specimens were imaged in dorsal, ventral and lateral views, together with a scale in millimeters. For the dorsal and ventral images, specimens were oriented with the occlusal plane of the molar teeth parallel to the camera focal plane. For lateral images the sagittal plane was aligned parallel to the focal plane. Images were saved as files, and landmarks digitized for the lateral view and both sides of the ventral and dorsal views, using TPS-DIGW (Rohlf, 1997). Specimen orientation and the chosen landmarks are shown in Fig. 1 and described in Table 2.

In order to avoid problems related to asymmetry and inflation of degrees of freedom resulting from digitizing both sides of a symmetrical structure, we analyze data for average half skulls. We used shape coordinates (Slice, 1994) to align the skull based on the midline landmarks - 1 and 5 for the

dorsal, and 1 and 7 for the ventral view. Sagittal plane landmarks were forced to lie exactly on a line, and the symmetrical landmarks were averaged. The entire number of landmarks was used only for comparison between centroid sizes, and the averaged right side was used for all subsequent analysis.

The averaged half skulls were then aligned using general least squares (GLS) superimposition, minimizing the summed squared distances between corresponding landmarks and the mean landmark positions of all of the specimens (the consensus) using TP-SRELW (Rohlf, 1998a), with the options “scale aligned 1”, and “projection orthogonal”. Centroid size (CS), the square root of the summed squared distances from all landmarks to the geometric centroid of the aligned coordinates, was obtained using TP-SREGW (Rohlf, 1998b), for each specimen in all three views.

We compared CS for the dorsal and ventral views, and for whole and averaged half skulls in order to examine the stability of centroid size as a “size” measurement (Bookstein, 1991). The ventral and dorsal views, as opposite sides of the same structure, should have similar, or at least highly correlated sizes.

Sexual dimorphism in size was analyzed by regressing centroid size on age, transformed to natural logarithms of (age in days plus 1), and comparing the slopes between the sexes with analysis of covariance (ANCOVA) and F-tests. A plot of CS against age showed a sigmoidal curve, while the log transformation of age provided a good approximation to a straight line relation.

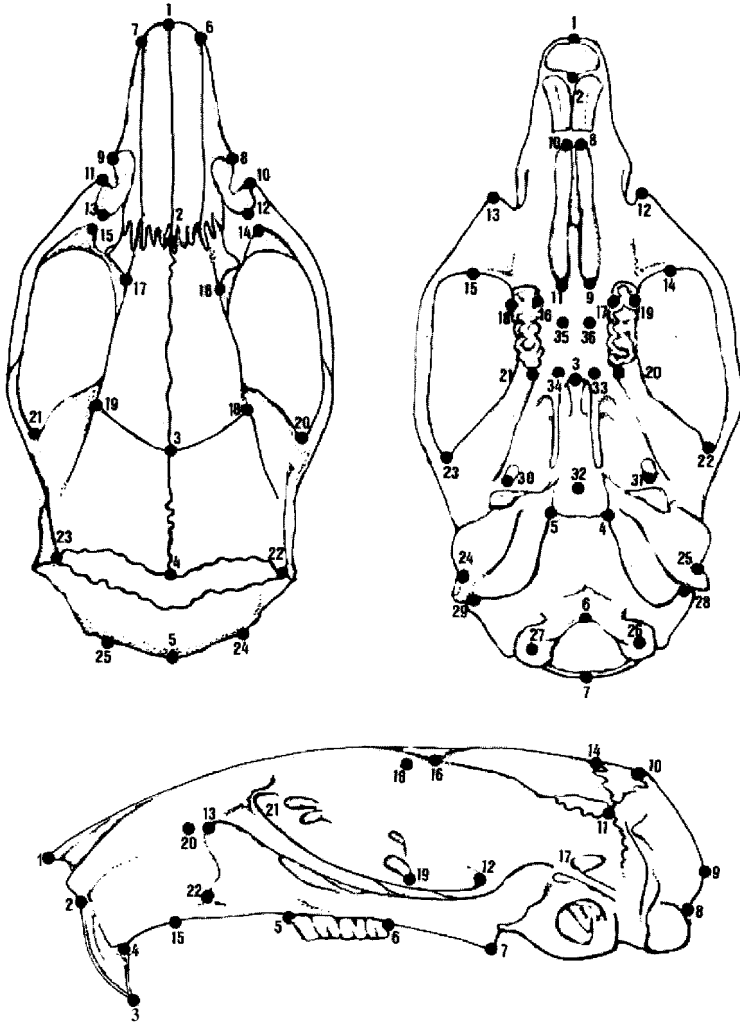


Figure 1 – Landmarks for dorsal, ventral and lateral view of *Calomys expulsius*

Shape differences were analyzed as a function of $\ln(\text{age}+1)$ for both sexes. Two-way analysis of variance (ANOVA) and multivariate analysis of variance (MANOVA) were used to test for age and sex differences, and age by sex interaction in aligned coordinates. Age was used as a covariate in a one way ANCOVA and multivariate analysis of covariance (MANCOVA) of **sex** to test for differences in slope for the two sexes.

Procrustes distance is the square root of the sum of squared differences between the position of the landmarks in two configurations superimposed by least squares at centroid size = 1 (Bookstein, 1996). We looked at Procrustes distances between mean landmark configurations for successive ages, as a way to measure the amount of shape change between ages. This procedure does not depend on the form of the growth curve

Table 2 – Description of the landmarks

Dorsal view*Sagittal plane*

1. tip of the nasals
2. nasal - frontal suture
3. frontal - parietal suture
4. midpoint of parietal - interparietal suture
5. rearmost point at supraoccipital

Right and Left sides

- 6 and 7. Most anterior points at nasal-premaxillary suture
- 8 and 9. Suture of premaxilla and maxilla over lachrymal capsule

Ventral view*Sagittal plane*

1. tip of nasal
2. tip of premaxilla on gnathic process
3. back of palatine
6. Anterior foramen magnum
7. Posterior foramen magnum
32. Middle of basilar fenestra

Right and Left sides

- 4 and 5. Lateral points of sphenoccipital suture
- 8 and 10. Front of incisive foramina
- 9 and 11. Back of incisive foramina
- 12 and 13. Front of zygomatic plate

Lateral view, right side

1. tip of nasal
2. upper point of incisors
3. tip of incisors
4. margin of the alveolus at the back of incisors
5. front of first molar
6. back of toothrow (over alveolus of last molar)
7. tip of pterygoid process
8. point above occipital condyle
9. point at the back of the skull over occipital
10. back of interparietal
11. Interparietal-occipital-squamosal intersection.

- 10 and 11. Anterior projection of zygoma
- 12 and 13. back of zygomatic notch
- 14 and 15. most anterior internal point of zygomatic arch
- 16 and 17. most medial point at interorbital constriction
- 18 and 19. Intersection of squamosal, parietal and frontal
- 20 and 21. Most anterior point on squamosal root of zygomatic arch
- 22 and 23. Intersection of parietal, interparietal and supraoccipital sutures
- 24 and 25. Back of the lateroccipital protuberances
- 14 and 15. Back of zygomatic plate
- 16 and 17. Protocone at M1
- 18 and 19. Lateral margin of M1 at the paracone
- 20 and 21. Back of toothrow (over the alveolus of last molar)
- 22 and 23. Front of glenoid fossa, on squamosal root of zygomatic arch
- 24 and 25. Back of external opening of auditory bullae
- 26 and 27. Middle of occipital condyles
- 28 and 29. Styloinastoid foramina at the posterior border of external auditory meatus
- 30 and 31. Back of the foramina ovale
- 33 and 34. Posterior palatal foramina
- 35 and 36. Anterior palatal foramina

12. Front of the squamosal root of the zygomatic
13. Front of the zygomatic plate
14. Front of interparietal
15. Premaxillar-maxillary suture
16. Lateral point at parietal-frontal suture
17. Upper point at the posterior margin of the hamular process of squamosal
18. Supraorbital foramen.
19. Dorsal intersection of alysphenoid and maxillary
20. Lateral rostral foramen (over maxillary)
21. Anterior point at maxillary root of zygomatic
22. Inferior margin of the infraorbital foramen

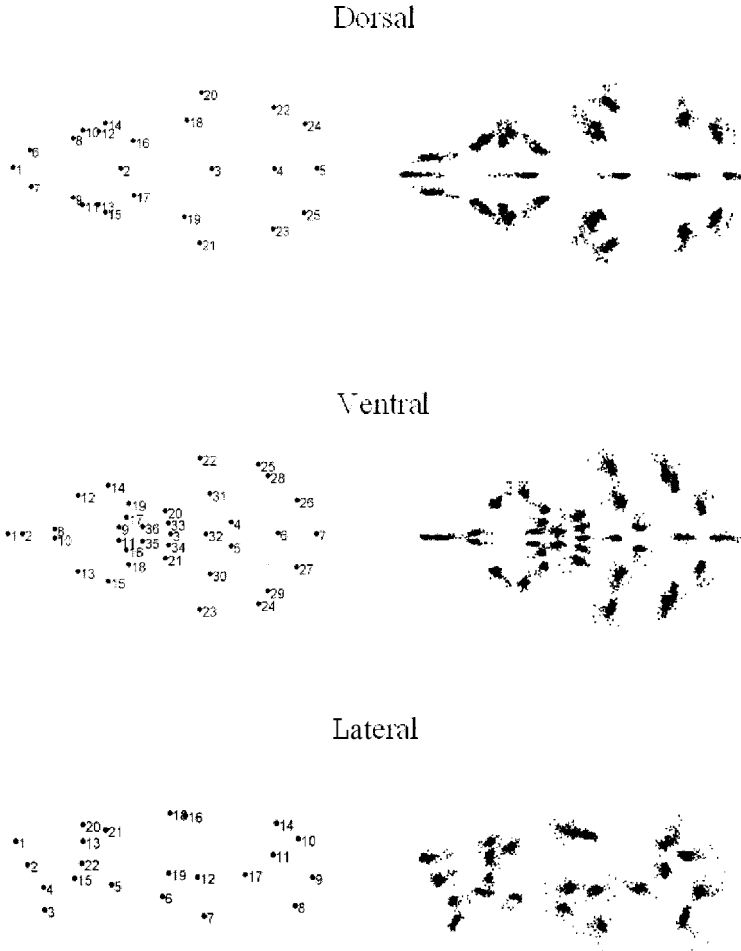


Figure 2 – Consensus and variation of all specimens aligned by GLS, for dorsal (top), ventral (center) and lateral view (bottom).

as does the method of partitioning Procrustes distance using regression applied by Monteiro et al. (1999).

We compared the Procrustes distances between mean shapes for males and females within each age class, as a way to determine sexual dimorphism in shape over ages. Visualization of differences between successive age classes and between sexes within each age class are presented as diagrams (figs. 4 and 5) using Morpheus et al. (Slice, 1999).

Shape variation throughout ontogeny was examined by comparing sum of squared Procrustes distances within each age about the mean shape for that age, grouping males and females, and dividing by the number of specimens at each age **minus** one to adjust for sample size. This statistic summarizes the scatter of shapes about the mean for each age for the aligned coordinates.

We used two approaches to try to find spatial patterns of developmental integration: the first

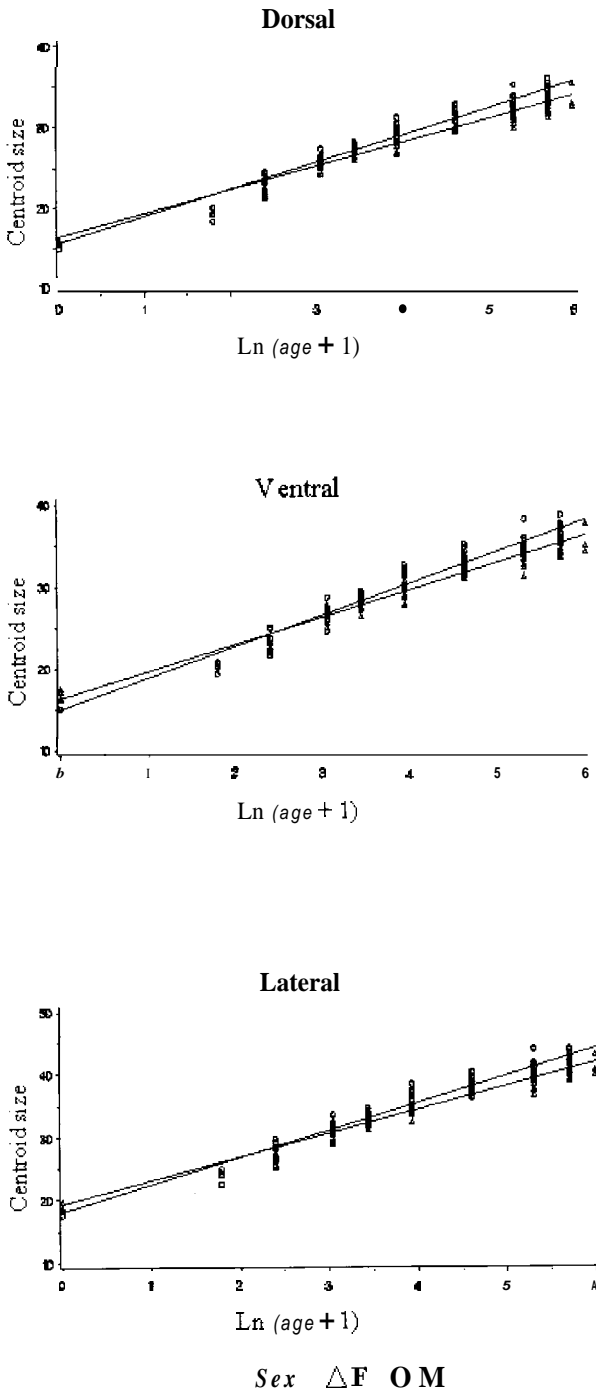


Figure 3 – Regression of centroid size on $\log_e(\text{age}+1)$.

explored covariation between subsets of the skull landmarks using partial least squares (PLS); and the second used the Zelditch et al. (1993) approach of looking at growth trajectories and superimposed concentration ellipses for each partial warp at each age.

In the PLS approach we chose subsets of landmarks as a simple way to divide the skull into potentially integrated units. We divided all three views into rostral and cranial sets of landmarks, and tested their integration. We also divided the lateral view into dorsal and ventral parts each containing portions of the rostral and cranial units. The bones that make up the face or viscerocranium originate from the neural crest, whereas the neurocranial vault and base—including frontal, parietal, occipital and sphenoid bones—are formed by the paraxial mesoderm cells (Noden, 1988). Moreover, preliminary inspection of the data has shown that facial growth is the main source of difference among ages, with the braincase growing at a slower rate. This is due to the fact that neurocranial growth is mainly com-

pleted during prenatal life, while the face continues to grow, under different hormonal control (Moore, 1981; Sara et al., 1981). Partial least squares (PLS) is a method similar to canonical correlation analysis, that can be used to explore patterns of covariation between two sets of variables. In contrast to canonical correlation, PLS does not weight the separate sets by the variation and covariation patterns within the sets (Rohlf and Corti, in press). Linear functions of the two sets are correlated if there is a pattern of covariation between the two sets. This correlation is tested using a permutation test (*op. cit.*). All statistical analyses were performed using SAS (1996).

RESULTS

The scatter and the consensus for all 169 aligned specimen\ are illustrated in Fig. 2, for both sides of the skull in ventral, dorsal, and lateral views. Most of the variation is age-related, but there is not much difference between the last two ages (200 and 300 days and older). The differences in growth rates

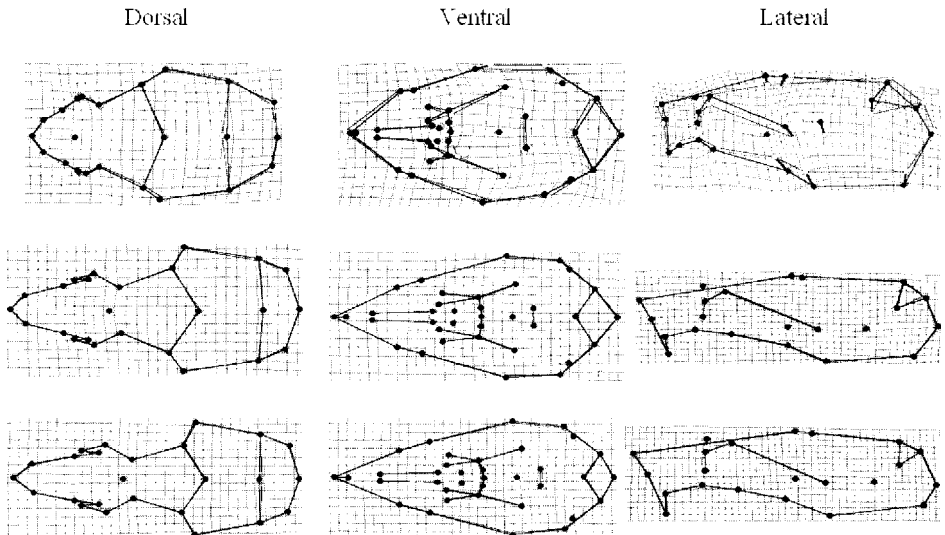


Figure 4 - Sexual dimorphism for 0 (top), 20 (center) and 100 days (bottom) for the dorsal, ventral and lateral views of the skull. ○ - female to ● male.

Table 3. Coefficients and slopes for the regression of centroid size on $\ln(\text{age}+1)$, and test for difference in slopes between sexes, with 1 and 165 df. Probability of a larger F by chance given as an exponent

Regression of Centroid Size on $\ln(\text{Age}+1)$						
	Dorsal		Ventral		Lateral	
	Intercept	Slope	Intercept	Slope	Intercept	Slope
Female	16.23±.33	2.932.08	16.36±.38	3.27±.09	19.31±.41	3.78±.10
Male	15.52±.47	3.31±.11	14.96±.50	3.82±.12	18.26±.57	4.28±.13
F test		9.05 ⁰⁰⁰³		15.16 ⁰⁰⁰¹		11.11 ⁰⁰¹

and shape changes between the rostrum and the braincase is easily seen, especially for the first 4 ages (Fig. 5 for 0 to 20 days). Comparison between centroid sizes for dorsal and ventral view showed correlation coefficients above 0.994, and for half and whole skulls in the same view the correlation coefficient was always above 0.999. Correlations of CS between lateral views and the other views, half or whole were all larger than 0.997.

Plotting CS against $\ln(\text{age}+1)$ made the relationship nearly linear (Fig. 3). There were

significant difference\ of slope between sexes for each view (Tab. 3). Males were smaller at an early age, but larger after 50 days and persisting as such into old age.

Preliminary analyses of covariance (ANCOVA) for aligned shape coordinates treating $\ln(\text{age}+1)$ as a covariate, with Bonferroni adjustments for all three views showed an interaction between age and sex for shape, the largest one for the lateral view, and gave different slopes for males and females. Treating age as a factor in a two-way ANOVA, which does not take into consideration

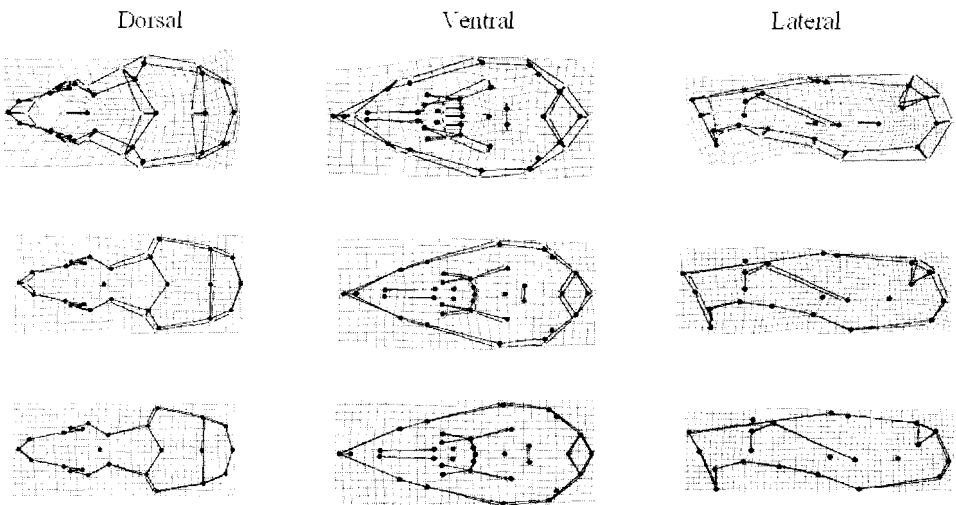


Figure 5 – Change in shape from 0-20 days (top), 20-100 days [center], and 100-300 days (bottom) for dorsal, ventral and lateral views. ○ - younger to ● - older.

the age ordering as does regression, there were still significant interactions between age and sex for all three views. Upon examination of the mean shapes for each sex and age it is clear that the interaction was entirely due to differences between sexes at the earliest ages (see Fig. 4 for differences in sex and Fig. 5 for changes from 0-20, 20-100 and 100-300 days). After 10 days, there is almost no difference in shape between the sexes. Unfortunately, the 0 and 5 day samples are very small, and differences between the two sexes could conceivably be attributed to the small sample sizes.

Examining both sexes together, most of the shape changes occur between 0 and 20 days (Fig. 5). In the dorsal view, there is a general elongation of the skull concentrated mainly in the rostrum, and a transverse narrowing of the skull across the frontals. A posterior shortening of the braincase occurs mainly between 0 and 5 days. These trends continue to diminish up to 100 days, after which the shape changes very little. The ventral view displays the same trend, especially from 0 to 5 days, with elongation of the snout and incisive foramen and posterior extension of the palate. Narrowing of the braincase can be perceived as the movement of the squamosal root of the zygomatic toward the sagittal plane and narrowing of the sphenoccipital suture. For the lateral view, Fig. 5 shows a forward movement of the zygomatic plate and infraorbital foramen, and a relative reduction of the interparietal. There is a change in the angle at the top of the skull between the frontal and parietal bones, and an overall narrowing from top to bottom.

Looking at Procrustes distances between successive ages (Fig. 6 top), for the three views, there is a general reduction of shape changes before 20 days. After that, shape changes are very small and constant. The strongest differences are concentrated between 0 and five days and five and ten days. There are more changes in the first 20 days for the lateral view than for dorsal and ventral views, reflecting shifts in the position of

foramina and the zygomatic plate, as well as an overall narrowing of the skull.

There are differences among the three views for Procrustes distances within ages (Fig 6 bottom): the initial distribution of landmarks around the mean for an age is least for the dorsal view, and it is more or less stable from 20 up to 300 days. A stronger decrease is evident for the ventral view, and it also stabilizes after 20 days. For the lateral view, Procrustes distance within ages declines up to 50 days, and then increases slightly at a higher level than for the other two views. Part of the changes we see in the beginning of development may be due to sexual dimorphism and/or small sample sizes at the earliest ages.

Integration - Attempts to find patterns of integration throughout post-natal development did not lead to clear results. Our partial least squares (PLS) approach for finding patterns of spatial integration during growth at each age depended of course on the way we subdivided the landmarks a priori. When we divided the landmarks into a rostrum and braincase subset for all three views, we found no significant correlation between the first linear combinations of the two subsets, within age groups for all age groups. This appears to be evidence that there is not a strong integration of the front and rear part of the skulls over individuals of the same age, but it is also possible that the power of the method might be insufficient for our sample sizes within ages to clearly detect changes in integration through age stages. PLS analysis for the entire data set of 169 skulls over all ages did show integration between the rostrum and braincase.

Ontogenetic trajectories (Zelditch et al., 1993) and bivariate distributions, and vectors depicting changes over age of uniform component and partial warp scores are plotted in Fig. 6 for dorsal, ventral, and lateral views. The ontogenetic trajectory forms roughly a 45 degree angle with the major axes of the bivariate ellipses, represented al-

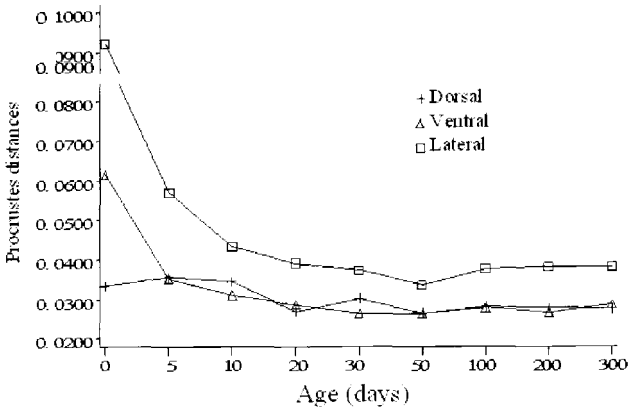
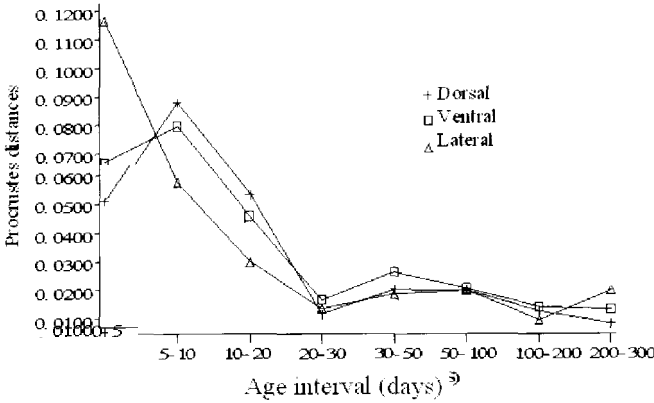


Figure 6 – Top - Change in Procrustes distance between consecutive ages; Bottom - Amount of Procrustes distance within each age divided by (n-1), where n is the number of specimens at each age.

so by the shear seen in the vectors on the various skull views. Note that the direction of shear in the ellipses changes at 10 days for dorsal and 5 days for ventral views. The lateral uniform component shows more of a vertical compression, and less overall shear. The first partial warps, are very local, as they should be a function of the closest landmarks, and involve the zygomatic plate for dorsal, first molar for ventral, and infra-orbital foramina for lateral views. The other partial warps represent functions of landmarks further apart, and are largely a function of landmark distribution.

The last partial warp shows the strongest trend with least change in the growth trajectory after 20 days, and at the same time the ellipses become more and more circular. Their pattern is similar to the relative warps, and summarizes the major trends in growth between the front and **sear** parts of the skull.

DISCUSSION

Irrespective of whether we can find new descriptive tools that are landmark dependent. landmarks in themselves give a richer description of the morphology than traditional measurements. When using traditional mea-

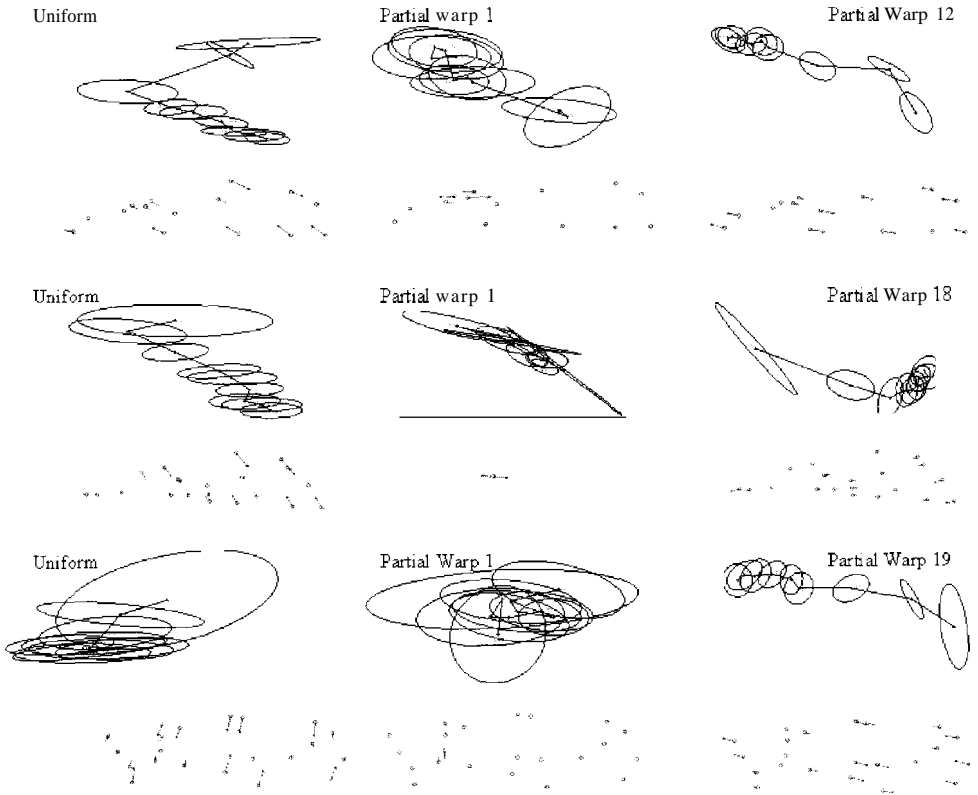


Figure 7 – Concentration ellipses (50%) and growth trajectory for dorsal, ventral, and lateral views together with thin plate spline vectors representing the shape changes from young to old specimens: Left - the uniform component; Middle - scores for the first partial warp; and Right - scores for the last partial warp.

surements, there is a tendency to include mainly directions of variation parallel to the skull axes; ignoring other directions. In addition, repeated measurements on the same axis often cover the same region more than once, therefore having built in dependencies. Landmarks are free of these constraints by their very nature. They can be partitioned in a large number of ways, either by an algorithm (e.g. partial warps) or a priori according to hypotheses of spatial integration. When we considered CS as a function of age for each view and for each sex separately, the regression lines of CS on $\ln(\text{age}+1)$ had significantly larger slopes for the males and higher intercepts for females (Tab. 3 and Fig.

3). This means that the males grew faster, exceeding the size of the females, which were larger at birth. The regression lines cross at about 10 days. Since sample size is small at age 0 days (1 male and 4 females) and 5 days (3 males and 1 female), it is not possible to determine if females are significantly larger at birth. Looking at distribution of centroid sizes over age, it is clear that males and females are more similar at 20 days (Fig. 3). Skull shape, on the other hand, is only different between the sexes at the earliest ages, and becomes very similar beyond 20 days (Fig. 4). Males beyond 30 days are larger, but have the same skull shape as females in the same age group. On average, males and

females will never have the same shape at the same centroid size, except where the lines for centroid size cross. In other words a female skull at 100 days will be on the average smaller than a male skull at 100 days, but both skulls will have the same shape. This difference in pattern of change for size and for shape suggests dissociation between the two parameters, with shape being the more conservative part of form.

Looking at the coefficient of variation of CS for each age, there is not a clear trend of reduction in variance for size from younger towards older ages. On the other hand, the "Procrustes within age" statistic, which demonstrates the amount of shape homogeneity at each age decreases for all three views, as shown in Fig. 6 (bottom). This trend of reduction in variation, or developmental regulation, detected for shape but not for size, is additional evidence of dissociation between the shape and size. There is a greater possibility of change occurring in size than in shape, which is not surprising, as changes in shape would require major rearrangements of functional structures that are more integrated during growth.

We did not find a clear pattern of integration for parts of the skull summarized by our landmarks. However, some parts of the skull must grow in an integrated fashion since birth, either because of common embryological origins or to exert common functions, in a pattern that might change with age. Moreover, looking at the means and distribution of our landmarks, it is easy to perceive different growth rates for the two parts we chose as subsets, the rostrum and the braincase. While the rostrum is growing faster, elongating with age, the braincase is becoming relatively smaller. Either our chosen landmarks were not the most appropriate to describe these patterns, or the way we divided them is not capturing integration between parts. It is not clear, either, how powerful the PLS technique is for sample sizes at each age with a large number of coordinates. Zelditch et al. (1993) suggested that the con-

centration ellipses over individuals using partial warp scores at each age relative to growth trajectories could be interpreted either as: random noise (ellipses as circles); regulation or canalization (ellipses getting progressively smaller); chreods (orientation of the greater axes of the ellipses with the trajectory); or opposition (greatest axis of ellipses perpendicular to the trajectory) of the landmarks involved in a specific partial warp. When applying the method to our data, we only found readily interpretable patterns for the uniform component and the most global partial warp (Fig. 7). This is expected, as they are the only components that look at the large scale changes, and therefore to overall pattern of developmental constraints. Partial warps partition localized shape differences from the ones involving a few close landmarks to large scale shape differences encompassing many landmarks (Fig. 7). The partial warps may show the same patterns of change in vastly different data sets, and not summarize the biological integration and development processes we are interested in describing.

ACKNOWLEDGEMENTS

We thank Nélio Pereira de Barros, and all the students that helped take care of the specimens at the Laboratório de Vertebrados. Francisca Cunha Almeida. Luciana Araripe and Julieta Freschi helped prepare the specimens, and Rodrigo Bastos, Flávia Rocha, Luciana Araripe and Diego Astúa de Moraes helped in fieldwork. Mr. Ivan Bastos allowed us to collect the field specimens in Fazenda Canoas. Francisca Almeida and Cibele Bonvicino identified the species. Many thanks also to Esteban Sarmiento and John Wahlert, who helped identify the structures under the landmark, and to the reviewers, who gave us many helpful critiques and suggestions to improve the clarity of the paper.

E.Hingst-Zaher was supported by a CAPES fellowship. CNPq, CAPES, FAPERJ, FUJB. and MMA (PROBIO) provided financial support.

REFERENCES

- Atchley, W.R., Plummer, A. and Riska, B., 1985a. Genetics of mandible form in the mouse. *Genetics*, 111: 555-577.
- Atchley, W.R., Plummer, A. and Riska, B., 1985b. Genetic analysis of size-scaling patterns in the mouse mandible. *Genetics* 111: 579-595.
- Bookstein, F.L., 1989. Principal warps: Thin plate splines and the decomposition of transformations. I.E.E.E. Trans. On Pattern Analysis and Machine Intelligence, 11: 567-585
- Bookstein, F.L., 1991. Morphometric tools for landmark data: geometry and biology. Cambridge Univ. Press, NY.
- Bookstein, F. L., 1996. Combining tools of geometric morphometrics. In: Marcus, L, Corti, M., Loy, A., Naylor G.J.P. and Slice, D. (eds.). *Advances in Morphometrics*. Plenum Press, NY: 131-151.
- Bookstein, F. L. 1998. A hundred years of morphometrics. *Acta Zool. Acad. Scient. Hung.*, 44: 7-59.
- Cheverud, J.M., 1995. Morphological integration in the saddle-backed tamarin (*Saguinus fuscicollis*) cranium. *Amer. Natur.* 145: 63-89.
- Cheverud, J.M. and Richtsmeier, J.T., 1986. Finite-element scaling applied to sexual-dimorphism in rhesus macaque (*Mucaca mulatta*) facial growth. *Syst. Zool.* 35: 381-399.
- Cheverud, J.M., Wagner, G.P. and Dow, M.M., 1989. Methods for comparative analysis of variation patterns. *Syst. Zool.*, 38: 201-213.
- Corti, M., 1993. Geometric morphometrics: an extension to the revolution. *TREE*, 8: 302-303.
- Hingst, E., 1995. Reprodução, crescimento e desenvolvimento em *Bolomys lasiurus* (Rodentia, Sigmodontinae). Dissertação de Mestrado, PPGE, UFRJ.
- Klingenberg, C. P. and Bookstein, F. L., 1998. Introduction to the symposium: putting the morphometric synthesis to work. *Acta Zool. Acad. Scient. Hung.* 44: 1-6.
- Leamy, L.J., Routman, E.J. and Cheverud, J.M., 1999. Quantitative trait loci for early- and late-developing skull characters in mice: a test of the genetic independence model of morphological integration. *Amer. Natur.*, 153: 201-214.
- Marcus, L. F. 1990. Traditional Morphometrics. In: Rohlf, F. J. and Bookstein, F. (eds.), *Proceedings of the Michigan Morphometrics Workshop*. Special Publications, The University of Michigan Museum of Zoology, Ann Arbor: 77-122.
- Marcus, L.F., Bello, E. and Garcia-Valdecasas, A., 1993. *Contributions to Morphometrics*. Monografias del Museo Nacional de Ciencias Naturales, 8. Madrid.
- Marcus, L, Corti, M., Loy, A., Naylor, G.J.P. and Slice, D., 1996. *Advances in Morphometrics*. Plenum Press, NY.
- Marcus, L. F., Frost, S. R., Bookstein, F., Reddy, D. and Delson, E., 1999. Comparison of landmarks among *Papio* skulls, with extension of Procrustes methods to ridge curves. *Amer. J. Phys. Anthr., Suppl.* 28: 190.
- Monteiro, L. R., Lessa, L. G. and Abe, A. S., 1999. Ontogenetic variation in skull shape of *Thrichomys upereoides* (Rodentia: Echimyidae). *J. Mamm.*, 80: 102-111.
- Moore, W. 1981. *The Mammalian Skull*. Cambridge University Press, Cambridge.
- Noden, D., 1988. Interactions and fates of avian craniofacial niesenchime. *Development*, 103 (suppl.): 121S-140S.
- Nonaka, K. and Nakata, M., 1984. Genetic variation and craniofacial growth in inbred rats. *J. Craniofac. Gen. Devel. Biol.* 4: 271-302.
- O'Higgins, P. and Jones, N., 1998. Facial growth in *Cercocebus torquatus*: an application of three-dimensional geometric morphometric techniques to the study of morphological variation. *J. Anat.*, 193: 251-272.
- Olson, E.C. and Miller, R.J., 1958. *Morphological Integration*. University of Chicago Press, Chicago.

- Riska, B., Atchley, W.R. and Rutledge, J.J., 1984. A genetic analysis of targeted growth in mice. *Genetics*, 107: 79-101.
- Rohlf, F.J., 1997. TpsDig, ver. 1.08. Dept. Ecology and Evolution. State University of New York at Stony Brook.
- Rohlf, F.J., 1998a. TpsRelW, ver. 1.16. Dept. Ecology and Evolution, State University of New York at Stony Brook.
- Rohlf, F.J., 1998b. TpsRegrW, ver. 1.13. Dept. Ecology and Evolution, State University of New York at Stony Brook.
- Rohlf, F.J., Bookstein, and F.L., 1990. Proceedings of the Michigan Morphometrics Workshop. Univ. Mich. Spec. Publ. 2. Ann Arbor, Michigan.
- Rohlf, F.J. and Marcus, L. F., 1993a. A revolution in morphometrics. *TREE*, 8: 129-132.
- Rohlf, F.J. and Marcus, L., 1993b. Geometric morphometrics: Reply to M. Corti. *TREE*, 8: 339.
- Sara, V., Hall, K. and Wetterberg, L., 1981. Fetal brain growth: a proposed model for regulation by embryonic somatomedin. In: Ritzen, M., Aperia, A., Hall, K., Larsson, A., Zetterberg, A. and Zetterstrom, A. (eds.) *Biology of normal human growth*. Raven, New York.
- SAS for Personal Computers, 1996. Release 6.12. SAS Institute, Cary, North Carolina.
- Slice, D. E. 1994., GRF-ND: Generalized rotational fitting of n-dimensional landmark data. Stonybrook, NY.
- Slice, D.E., 1998. Morpheus et al.: software for morphometric research. Revision 01-30-98. Department of Ecology and Evolution, State University of New York, Stony Brook, New York.
- Tanner, J.M., 1963. Regulation of growth in size in mammals. *Nature*, 199: 845-850.
- Voss, R. S., Marcus, L. F. and Escalante, P., 1990. Morphological evolution in murid rodents I. Conservative patterns of cranio-metric covariance and their ontogenetic basis in the Neotropical genus *Zygodontomys*. *Evolution* 44: 1568-1587.
- Waddington, C. H., 1968. The basic ideas of Biology. In C Waddington, H. (ed.). *The evolution of an Evolutionist*. Cornell Univ. Press, Ithaca
- Wright, S., 1921. Correlation and causation. *J. Agric. Res.* 20: 557-585.
- Wright, S., 1968. *Evolution and the Genetics of Populations. I. Genetic and Biometric Foundations*. University of Chicago Press. Chicago.
- Zelditch, M.L., 1988. Ontogenetic variation in patterns of phenotypic integration in the laboratory rat. *Evolution*, 42: 28-41.
- Zelditch, M.L. and Carmichael, A.C., 1989. Growth and intensity of integration through postnatal growth in the skull of *Sigmodon fulviventer*. *J. Mamm.* 70: 477-484.
- Zelditch, M.L., Bookstein, F.L. and Lundri-gan, B.L., 1992. Ontogeny of integrated skull growth in the cotton rat *Sigmodon fulviventer*. *Evolution*, 46: 1164-1180.
- Zelditch, M.L., Bookstein, F.L. and Lundri-gan, B.L., 1993. The ontogenetic complexity of developmental constraints. *J. Evol. Biol.*, 6: 621-641.